

## Article

# Combining Ultraviolet Photolysis with In-Situ Electrochemical Oxidation for Degrading Sulfonamides in Wastewater

Zhijie Zheng<sup>1</sup>, Julin Yuan<sup>2</sup>, Xinwei Jiang<sup>1</sup>, Gang Han<sup>1</sup>, Yufang Tao<sup>3</sup> and Xiaogang Wu<sup>1,\*</sup>

<sup>1</sup> School of Urban Construction, Yangtze University, Jingzhou 434103, China; zzsocial@foxmail.com (Z.Z.); a26818710852022@163.com (X.J.); hh123gang@163.com (G.H.)

<sup>2</sup> Key Laboratory of Healthy Freshwater Aquaculture, Ministry of Agriculture and Rural Affairs, Key Laboratory of Fish Health and Nutrition of Zhejiang Province, Zhejiang Institute of Freshwater Fisheries, Huzhou 313001, China; yuanjulin1982@163.com

<sup>3</sup> College of Chemistry & Environmental Engineering, Yangtze University, Jingzhou 434103, China; taoyufang@yangtzeu.edu.cn

\* Correspondence: wxgglobes@163.com

**Abstract:** Ultraviolet photolysis (UVC, 254 nm) was coupled with an electrochemical oxidation process to degrade three kinds of veterinary sulfonamide (sulfamethazine [SMZ] tablets, sulfamonomethoxine [SMM] tablets, and compound sulfamethoxazole [SMX] tablets). The treatment was applied using a flat ceramic microfiltration membrane to study the effects of photocatalysts. The effectiveness of degradation of the three sulfonamides was evaluated under different conditions. Dissolved oxygen was provided via aeration, but this resulted in a large decrease in the degradation effectiveness due to the inhibition of free chlorine electrogeneration. The photocatalysts had no promotional effect on sulfonamide removal from wastewater due to reduced UV penetration. Because of the different distribution coefficients of sulfonamides, UV irradiation had different effects on different sulfonamide species. For SMZ and SMM, anionic species exhibited a higher degradation rate, whereas for SMX, degradation was most effective for neutral species. In addition, the free chlorine yield increased as the pH increased. Free chlorine conversion reactions occurred under UV irradiation, with the reactions possibly restrained by sulfonamides. Reactive chlorine species promoted SMM degradation. Compared to UV irradiation or electrochemical oxidation alone, the UV/in-situ electrochemical oxidation process was more effective and is suitable for treating real wastewater under various environmental pH levels.

**Keywords:** ultraviolet photolysis; in-situ electrochemical oxidation; sulfonamides; aeration



**Citation:** Zheng, Z.; Yuan, J.; Jiang, X.; Han, G.; Tao, Y.; Wu, X. Combining Ultraviolet Photolysis with In-Situ Electrochemical Oxidation for Degrading Sulfonamides in Wastewater. *Catalysts* **2022**, *12*, 711. <https://doi.org/10.3390/catal12070711>

Academic Editor: Ewa Kowalska

Received: 14 June 2022

Accepted: 25 June 2022

Published: 29 June 2022

**Publisher's Note:** MDPI stays neutral with regard to jurisdictional claims in published maps and institutional affiliations.



**Copyright:** © 2022 by the authors. Licensee MDPI, Basel, Switzerland. This article is an open access article distributed under the terms and conditions of the Creative Commons Attribution (CC BY) license (<https://creativecommons.org/licenses/by/4.0/>).

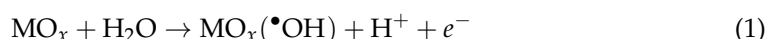
## 1. Introduction

As an environmentally sustainable wastewater-treatment technology, ultraviolet (UV)-based techniques have been widely used for sewage treatment due to their advantages of high inactivation efficiency against pathogenic microorganisms, limited production of disinfection by-products (DBPs), small spatial requirements, and convenience of operation and maintenance [1]. In addition to inactivating the DNA and/or RNA of microorganisms in water, UV light can also decompose many micropollutants through photochemical reactions [2].

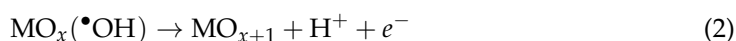
Electrochemical advanced oxidation processes have also been widely used for wastewater treatment, including the removal of antibiotics [3,4]. Electrochemical advanced oxidation processes include electrocoagulation, electrochemical oxidation, electrochemical reduction, photo-assisted electrochemical degradation, and electro-Fenton process [5–7]. In these processes, electrochemical oxidation is achieved mainly by the adsorption of hydroxyl radicals ( $\bullet\text{OH}$ ) on the surface of the anode (i.e., direct oxidation or anode oxidation) or the dispersal of various kinds of active substances in the solution system (i.e., indirect

oxidation), including active chlorine species, hydrogen peroxide (H<sub>2</sub>O<sub>2</sub>), ozone (O<sub>3</sub>), and persulfate [8,9].

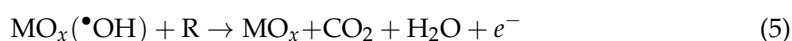
In electrochemical oxidation, the degradation of organics mainly occurs through direct and indirect oxidation. In direct oxidation, pollutants can be directly oxidized at the anodes through the generation of physically adsorbed “active oxygen” (adsorbed •OH) or chemisorbed “active oxygen” (oxygen in the oxide lattice, MO<sub>x+1</sub>) [10]. Furthermore, anodes can be divided into “active anodes” and “non-active anodes” [11]. First, the following reaction occurs:



This is the process by which water molecules break down near the anode to form adsorbed •OH. The following process then occurs at the “active anode”:

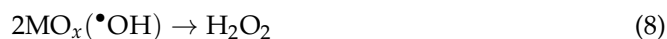
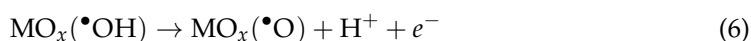


The redox couple MO<sub>x+1</sub>/MO<sub>x</sub> acts as a mediator in the oxidation process (Equation (3)), in which only the partial oxidation of organics can be achieved. The reaction competes with the side reaction of oxygen evolution (Equation (4)), which is due to the chemical decomposition of the higher oxide (MO<sub>x+1</sub>). Hydroxyl radicals play a major role in the oxidation of organics at the “non-active anode,” which can result in complete conversion to CO<sub>2</sub> as follows:

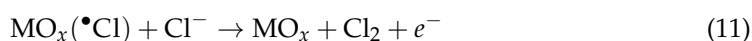
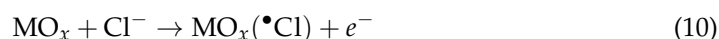


Therefore, the “active anode” is a good catalyst for an oxygen evolution reaction, which may be related to the oxygen evolution overpotential [10]. The lower the oxygen evolution overpotential, the less effective the oxidation of organics due to the oxygen evolution side reaction (Equation (4)).

However, it is difficult to achieve good removal of organics using only direct oxidation. Indirect oxidation also plays an important role in the electrochemical process. Active oxygen species are generated near the anode through an electrochemical process as follows [12]:

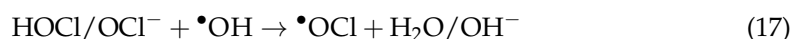


When the solution contains chloride ions (Cl<sup>−</sup>), active chlorine species such as hypochlorous acid (HOCl), hypochlorite (OCl<sup>−</sup>), and chlorine (Cl<sub>2</sub>) can also be produced electrochemically, and the oxidation of organics is accomplished [13,14]. In the presence of Cl<sup>−</sup>, the following reactions can occur [15]:



HOCl can dissociate to  $\text{OCl}^-$  through Equation (14), with the HOCl/ $\text{OCl}^-$  ratio dependent on the pH. Due to the presence of  $\text{Cl}^-$ , oxygen evolution (Equation (4)) may be inhibited [9].

When exposed to UV light, free chlorine can be converted into other radicals as follows [16–18]:



Reactive chlorine species ( $\bullet\text{Cl}$ ,  $\bullet\text{ClO}$ , and  $\bullet\text{Cl}_2^-$ ) work together with  $\bullet\text{OH}$  to degrade organics in this UV/chlorine system, with the reactions with organics featuring one-electron oxidation, H-abstraction, and the addition of unsaturated C–C bonds [19–21].

Due to the various advantages of UV photolysis and electrochemical oxidation, combined treatment processes have been investigated. Kishimoto developed a treatment process in which UV photolysis was combined with electrochemical oxidation and achieved stable degradation of 1,4 dioxane [16]. However, the electrolysis part of the process was separated from UV lamp exposure in their experiment, such that only indirect oxidation was applied. It still provided a possible treatment for use in further experiments. Furthermore, the photocatalyst could be used for the presence of membrane [22,23]. The photocatalyst was retained on a microfiltration membrane, which could not only separate both photocatalysts and some intermediate by-products but also enabled the continuous reuse and recirculation of the photocatalyst [24,25].

This study attempted to combine UV photolysis (UVC, 254 nm) with in-situ electrochemical oxidation and investigated the effectiveness of this process for the treatment of wastewater containing veterinary sulfonamides. Additionally, a flat ceramic microfiltration membrane was also incorporated into the system to determine the effect of photocatalysts. Tap water was used to prepare simulated wastewater, and the influence of different factors was evaluated.

## 2. Results and Discussion

### 2.1. Influence of Different Aeration Rates

Aeration rates of 0, 15, 30, and 55 L/min were used to evaluate the influence of different dissolved oxygen concentrations on the degradation of sulfonamides. With a high current and  $\text{Cl}^-$  concentration (Figure 1a), there was no significant promotion of sulfonamide degradation under different aeration conditions (aeration rate of 15, 30, or 55 L/min). Under all aeration conditions, sulfonamide degradation was greatly decreased compared with the degradation achieved under no aeration (aeration rate of 0 L/min), which had no significant differences of degradation rate constant (Figure 1b). It could be the inhibition of electrogenerated free chlorine.

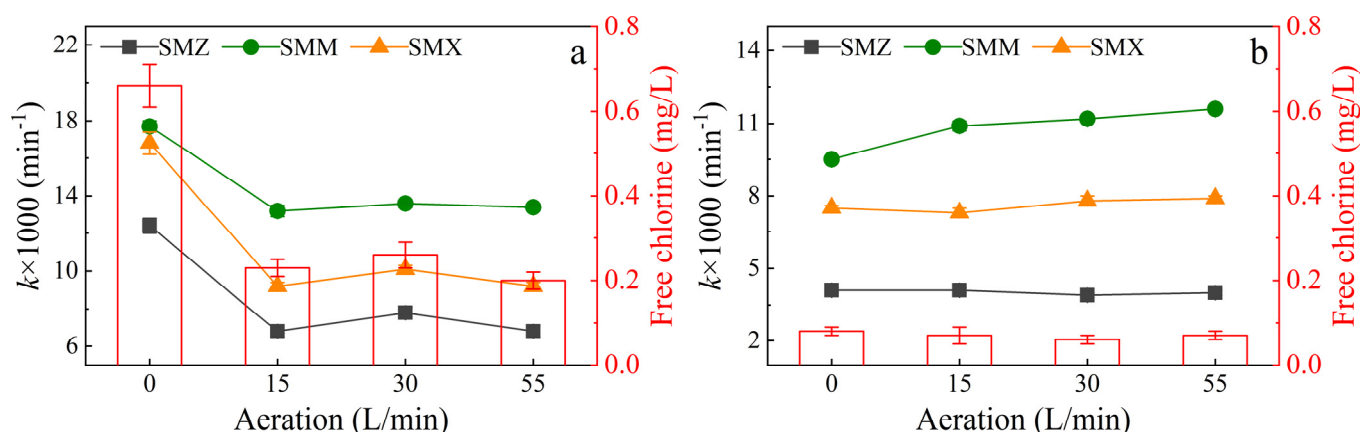


**Figure 1.** Pseudo-first-order kinetic rate constant ( $k$ ) for sulfonamide degradation after 120 min. Conditions: aeration rate of 0, 15, 30, or 55 L/min, UV power of 48 W, and initial pH of 8.3. (a)  $Cl^-$  concentration of 50 mg/L and current of 1.8 A (4.8 mA/cm<sup>2</sup>). (b)  $Cl^-$  concentration of 20 mg/L and current of 1.0 A (2.7 mA/cm<sup>2</sup>).

## 2.2. Influence of $Cl^-$ Concentration and Aeration

As shown in Figure 2, two groups of experiments were conducted at aeration rates of 0 and 30 L/min and under different  $Cl^-$  concentrations. With no aeration (0 L/min), the  $k$  value increased steadily with increasing  $Cl^-$  concentration, which was due to the behavior of free chlorine. However, there was no obvious variation under aeration at 30 L/min, and the  $k$  value followed an interesting pattern across the different  $Cl^-$  concentrations. Under a low  $Cl^-$  concentration, the best degradation with aeration was observed for SMM. It could be the SMM was favored to react with  $\cdot OH$  [26] produced by anode or UV/chlorine conversion reactions (Equations (15)–(19)), and aeration had accelerated this process. While the SMX degradation had no obvious difference, indicating that the aeration promotion effect was offset by the decrease in free chlorine. As the  $Cl^-$  concentration increased, the electrogeneration of chlorine was accelerated and electrochemical indirect oxidation was enhanced, resulting in efficient removal at a high  $Cl^-$  concentration.

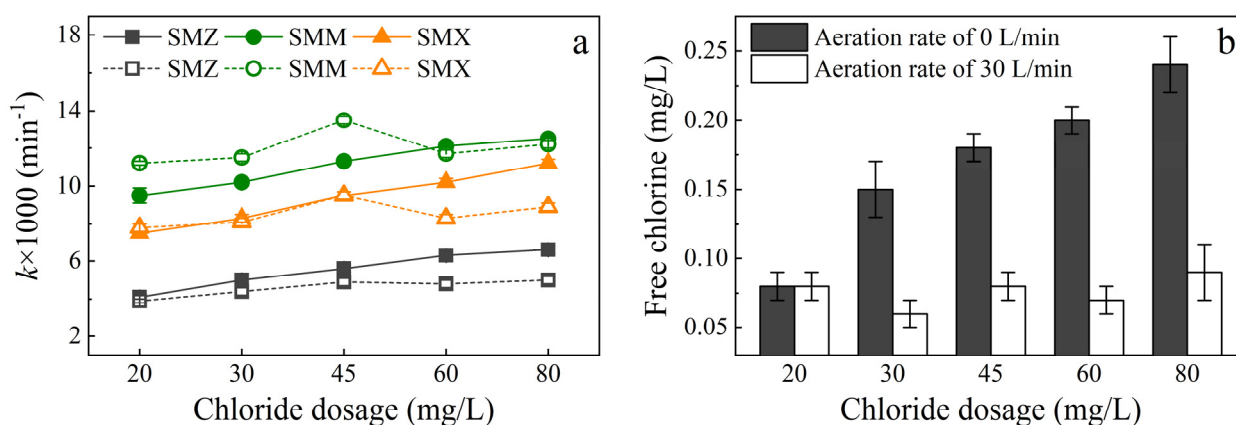


**Figure 2.** Effect of  $Cl^-$  concentration on sulfonamide degradation. Conditions:  $Cl^-$  concentration from 20 to 80 mg/L, aeration rate of 0 or 30 L/min, UV power of 48 W, current of 1.0 A (2.7 mA/cm<sup>2</sup>), and initial pH of 8.3. (a) The  $k$  value for sulfonamide degradation at different  $Cl^-$  concentrations. Solid points represent an aeration rate of 0 L/min and empty points represent an aeration rate of 30 L/min. (b) The free chlorine concentration at 120 min for different  $Cl^-$  concentrations.

This phenomenon confirmed our assumption that aeration would inhibit the electrogeneration of free chlorine at the anode, which could be attributed to most of the chlorine being precipitated by aeration after electrogeneration and therefore not participating in

the formation of free chlorine. Consequently, an assessment of the potential effects on the hydrodynamics of aeration was necessary.

### 2.3. Influence of Different Systems and Aeration

Experiments were conducted using different treatment systems with aeration rates of 0 and 30 L/min. Figure 3 shows the impact of different treatments on sulfonamide degradation. The results showed that the aeration rate mainly had an impact on electrolysis but had little influence on UV photolysis, only SMM was more affected by photodegradation than other two substances, especially under an aeration rate of 30 L/min which could increase the mass transfer effect. In addition, the aeration had a slight promotional effect on SMM degradation. However, because the effect was small, the treatment was not cost-effective given the energy consumed to provide aeration.

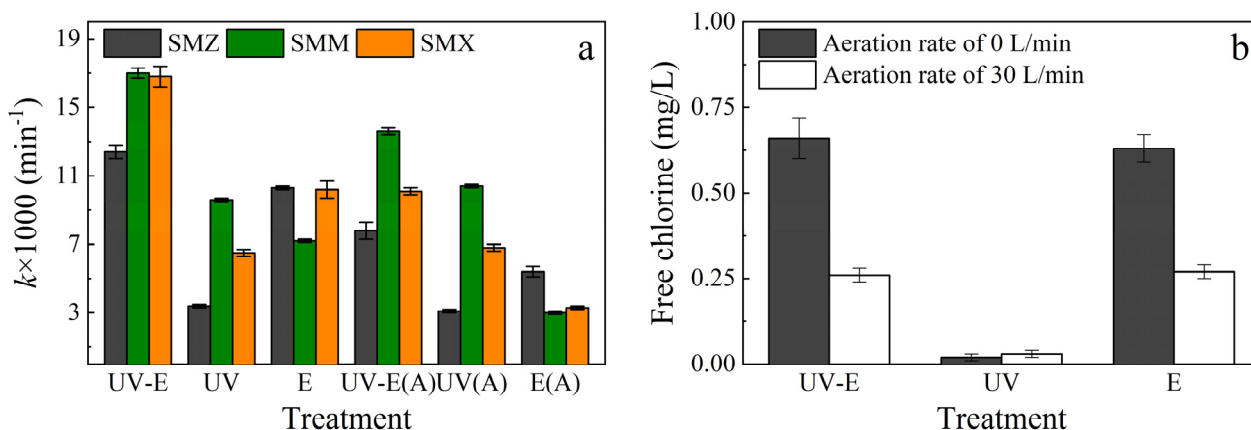


**Figure 3.** Effects of different treatments on sulfonamide degradation. Conditions: Cl<sup>-</sup> concentration of 50 mg/L, aeration rate of 0 or 30 L/min, UV power of 48 W, current of 1.8 A (4.8 mA/cm<sup>2</sup>), and initial pH of 8.3. UV-E: UV irradiation and electrolysis; UV: UV irradiation only; E: electrolysis only. (a) The  $k$  value for sulfonamide degradation with different treatments. “(A)” represents an aeration rate of 30 L/min. (b) The free chlorine concentration at 120 min with different treatments.

Figure 3a shows the  $k$  values for sulfonamide degradation with different treatments. SMZ and SMX were preferentially degraded via electrolysis, whereas SMM was preferentially degraded via UV treatment. The effectiveness of sulfonamide degradation varied among the different systems, which was caused by selective oxidation due to the disposal methods used for organics [2,27–29]. In this experiment, UV irradiation oxidation and indirect electrochemical oxidation were the dominant factors. The amount of direct oxidation at the anode was relatively small with aeration rates of 0 and 30 L/min in the electrolysis-only system.

### 2.4. Influence of Photocatalysts

The removal of organic contaminants with photocatalysts (TiO<sub>2</sub> and ZnO) was investigated in systems that employed photoactivated semiconductors to degrade low levels of pollutants in the environment [30]. Taking TiO<sub>2</sub> for example, two products of valence band holes (h<sup>+</sup>) and conduction band electrons (e<sup>-</sup>) are generated under UV irradiation as follows:



For these two reaction products, h<sup>+</sup> is a powerful oxidant and e<sup>-</sup> is a good reductant. Both can migrate to the surface of TiO<sub>2</sub>, and through the generation of •HO and •O<sub>2</sub><sup>-</sup> to facilitate the degradation of pollutants [31,32].

In our experiments, TiO<sub>2</sub> and ZnO were applied in two systems (UV-E and UV), and a control group was established. Each photocatalyst was retained on a microfiltration membrane, which could not only separate both photocatalysts and some intermediate by-products but also enable the continuous reuse and recirculation of the photocatalyst [24,25].

Unfortunately, neither of the photocatalysts promoted degradation (Figure 4). Even with a high concentration, TiO<sub>2</sub> was less effective than ZnO in the UV system, indicating that UV irradiation might have been inhibited. Although UV (254 nm) irradiation had a strong effect on the degradation of sulfonamides, the photocatalysts reduced UV penetration, which weakened the photolysis of sulfonamides. At the same time, it appeared that there was no obvious degradation effect of UV/photocatalysts on sulfonamides. The minimal impact of the photocatalysts was insufficient to compensate for the reduced transmittance being imparted to the system by the photocatalysts. However, it may be possible to use photocatalysts for the treatment of other organics. It has been reported that UV (254 nm) irradiation with TiO<sub>2</sub> was effective for the degradation of dimethyl phthalate, which is relatively nonreactive to UV irradiation and free chlorine unlike sulfonamides [33]. Therefore, photocatalysts should be added according to the type of organic material that needs to be removed.

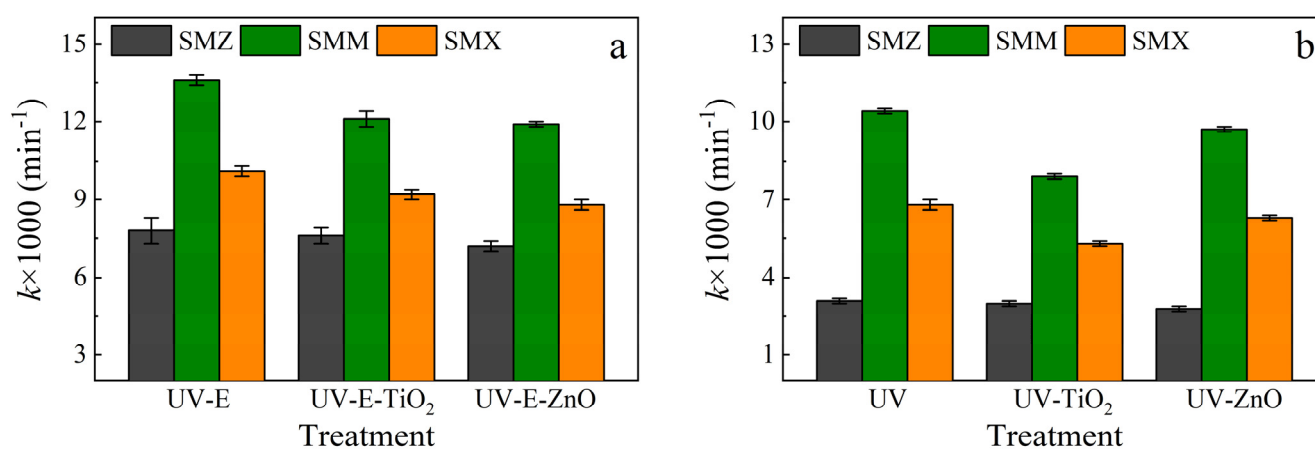


**Figure 4.** Effects of photocatalysts on sulfonamide degradation. Conditions: Cl<sup>−</sup> concentration of 50 mg/L, aeration rate of 30 L/min, UV power of 48 W, current of 1.8 A (4.8 mA/cm<sup>2</sup>), addition of TiO<sub>2</sub> (0.5 g/L) or ZnO (0.1 g/L), and initial pH of 8.3. UV-E: UV irradiation and electrolysis, UV: UV irradiation only, and E: electrolysis only. (a) The  $k$  value for sulfonamide degradation in UV-E systems. (b) The  $k$  value for sulfonamide degradation in UV-only systems.

## 2.5. Influence of Initial pH

### 2.5.1. Effects of Initial pH and Different Treatments on Sulfonamide Degradation

The effectiveness of sulfonamide degradation at different initial pH values in the different systems was investigated, and the results are shown in Figure 5. The effectiveness of sulfonamide degradation under different initial pH conditions and treatments followed a characteristic pattern. As the initial pH increased, the SMZ degradation efficiency followed a similar trend in the three systems, with a rapid increase to reach an optimal value at pH 8.3 followed by a decrease (Figure 5a). The E system provided the most efficient environment for SMZ degradation under alkaline conditions. Figure 5b shows that SMM degradation followed a similar trend to that of SMZ when the initial pH was raised. For SMM degradation, almost the same trend was observed in both the UV-E and UV systems with changes in pH, whereas the E system was less impacted by pH. Similar to SMZ degradation, alkaline conditions led to an optimal result for SMM degradation, with degradation almost twice as effective as under acidic conditions (pH 5.3). By contrast, SMX degradation followed a completely different pattern (Figure 5c). The  $k$  values for both the UV-E and UV systems decreased substantially when the pH ranged from acidic conditions, but the opposite effect was observed for the E system. In all systems, there was a slow reduction in efficiency under alkaline conditions. The total degradation rate in the UV-E and E systems initially increased and then decreased as the pH increased. The optimal degradation rate in the UV-E system was 84% at an initial pH of 8.3 for a 120-min reaction (Figure 5d), with the corresponding value being 66% in the E system. There was

little variation in degradation efficiency with pH in the UV system, with degradation rates remaining around 50%.

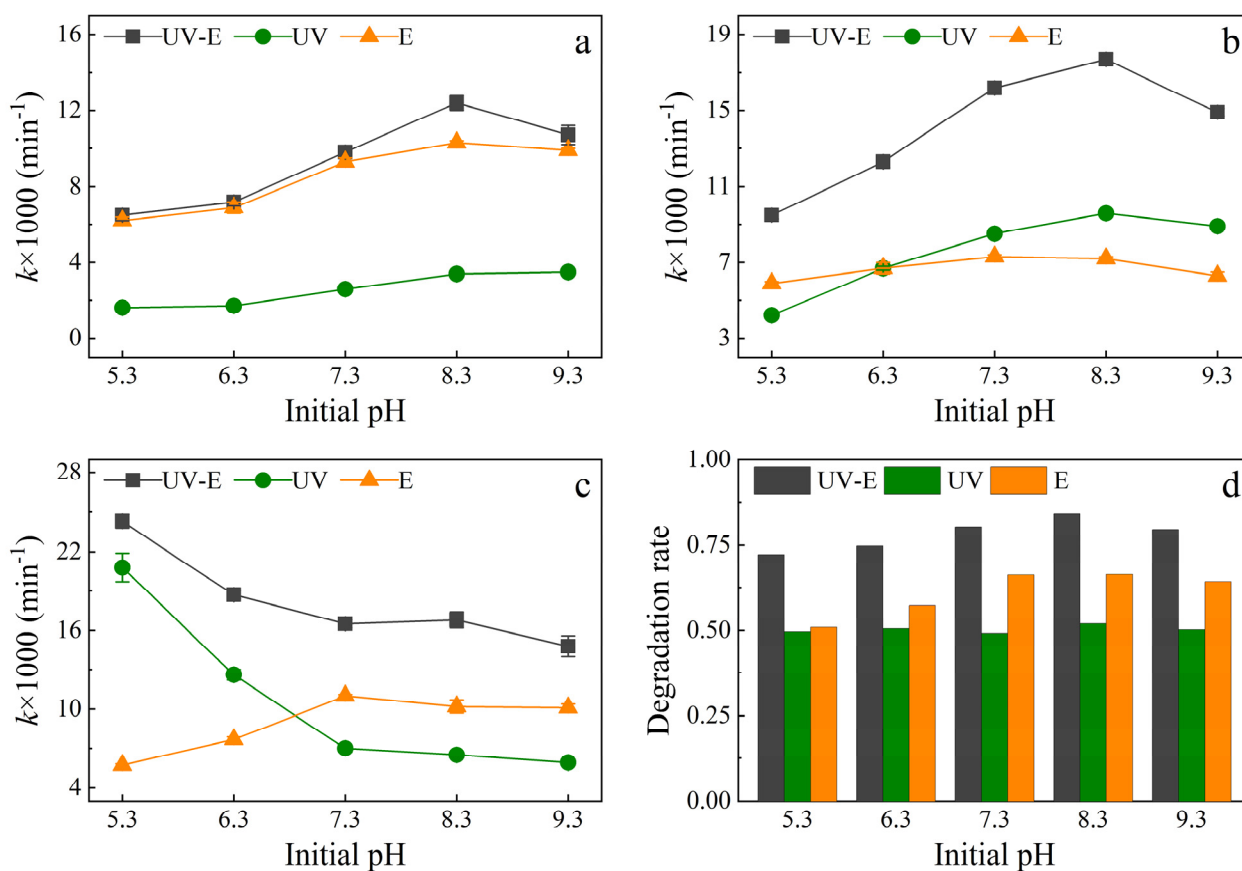


**Figure 5.** Effect of different initial pH on sulfonamide degradation. Conditions: Cl<sup>-</sup> concentration of 50 mg/L, no aeration, UV power of 48 W, current of 1.8 A (4.8 mA/cm<sup>2</sup>), and initial pH of 8.3. UV-E: UV irradiation and electrolysis, UV: UV irradiation only, and E: electrolysis only. The  $k$  values for (a) SMZ, (b) SMM, and (c) SMX. (d) The total degradation rate in the different systems.

These phenomena could be attributed to the differences in the distribution of sulfonamides and free chlorine under different pH conditions (Figure A1), and the sulfonamide species (cationic, neutral, and anionic) underwent different reaction rates with UV photolysis [34] and active chlorine species (HOCl, OCl<sup>-</sup>) [35]. The sulfonamide species and HOCl distributions are shown in Figure 6. Cationic sulfonamide species were negligible in the pH range of 5.3–9.3. Thus, the main species of concern were neutral and anionic in this experiment. For the three sulfonamides, their neutral species increased as the pH increased. The proportions under various pH conditions differed, which will be explained in the subsequent sections.

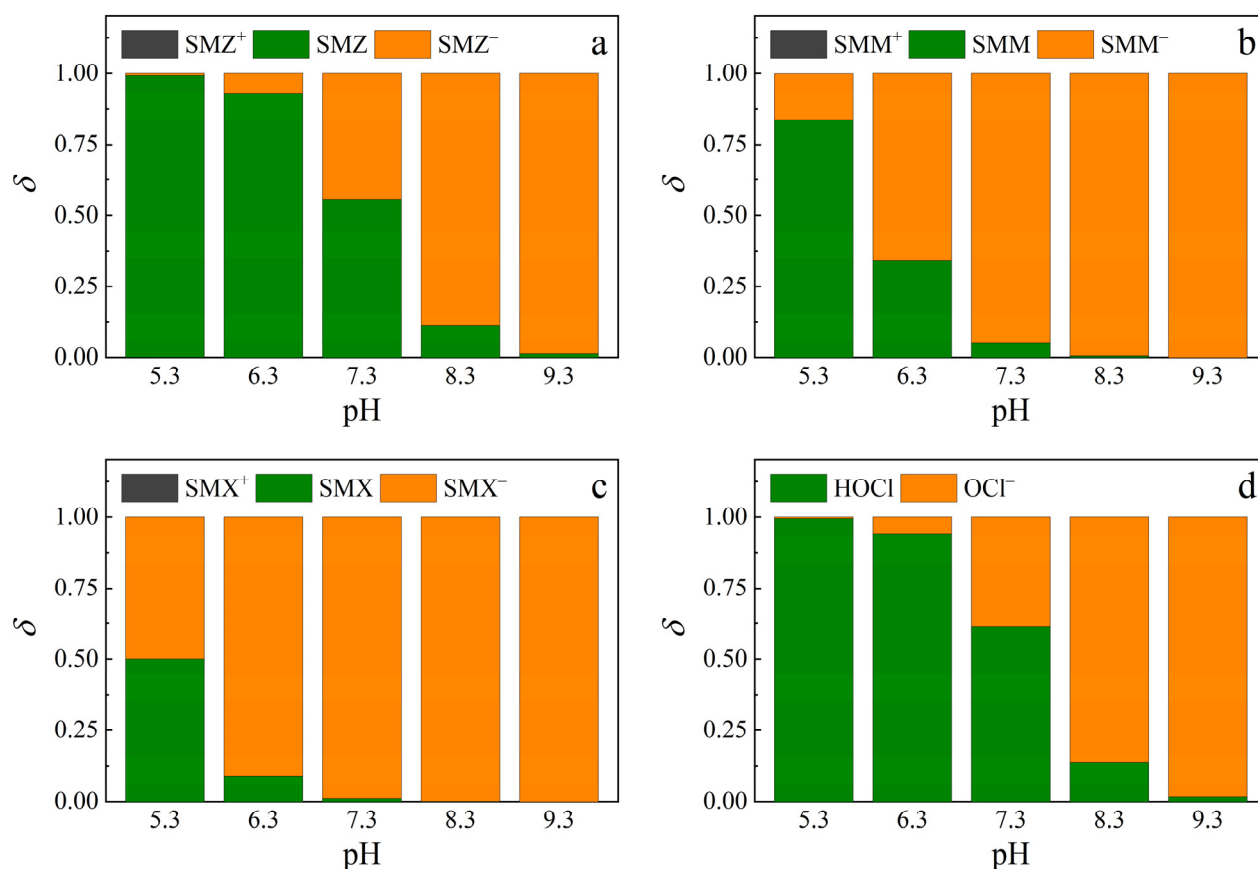


**Figure 6.** Distribution coefficients ( $\delta$ ) of sulfonamides (“+”, no mark, and “-” represent cationic, neutral, and anionic species, respectively) and HOCl at different pH. Distribution of (a) SMZ species, (b) SMM species, (c) SMX species, and (d) chlorine species.

### 2.5.2. UV Irradiation Photolysis of Sulfonamides

The pH variation was small ( $\pm 0.2$ ) during the experiment with the UV system, and the degradation tendency of the three sulfonamides in the UV system was similar to that reported previously [34,36]. The degradation effectiveness of UV photolysis differed among the different species of sulfonamides and was related to their molar absorption coefficient, as defined by the Lambert-Beer Law as follows:

$$A = \epsilon cl, \quad (21)$$

where  $A$  is the solution absorbance at 254 nm,  $\epsilon$  is the molar absorption coefficient (mol/cm),  $c$  is the sulfonamide concentration (10  $\mu\text{mol/L}$ ), and  $l$  is the path length (1 cm). The overall absorbance of the sulfonamide solution is equal to the sum of the specific absorbance of sulfonamide species (cationic, neutral, and anionic):

$$A = A_{\text{cationic}} + A_{\text{neutral}} + A_{\text{anionic}} \quad (22)$$

Similarly, the  $\epsilon$  value can be easily derived as:

$$\epsilon = \epsilon_{\text{cationic}}\delta_{\text{cationic}} + \epsilon_{\text{neutral}}\delta_{\text{neutral}} + \epsilon_{\text{anionic}}\delta_{\text{anionic}}, \quad (23)$$

where  $\delta$  is the distribution coefficient. Because the cationic value was negligible in this experiment, Equation (23) can be simplified as follows:

$$\epsilon = \epsilon_{\text{neutral}}\delta_{\text{neutral}} + \epsilon_{\text{anionic}}\delta_{\text{anionic}} \quad (24)$$

At a certain pH, the overall  $k$  (pseudo-first-order kinetic rate constant) for a sulfonamide is equal to the sum of the specific  $k$  for each sulfonamide species (cationic, neutral, and anionic) multiplied by its corresponding  $\vartheta$ . This was proposed by Lian [34] and is written as follows:

$$k = k_{\text{cationic}}\delta_{\text{cationic}} + k_{\text{neutral}}\delta_{\text{neutral}} + k_{\text{anionic}}\delta_{\text{anionic}}, \quad (25)$$

Equation (25) can be simplified to give:

$$k = k_{\text{neutral}}\delta_{\text{neutral}} + k_{\text{anionic}}\delta_{\text{anionic}} \quad (26)$$

The overall  $\varepsilon$  value was determined through UV-vis detection of each sulfonamide in solution at a certain pH (Figure A2), and the  $\varepsilon$  value of each species was easily calculated according to their  $\vartheta$  value from Equation (24) through regression analysis using Origin 9.0 software. Hence, the  $k$  value could also be determined using Equation (26). The specific parameters of the sulfonamide species are shown in Table 1, and the model fitting and measurement results are shown in Figure 7.

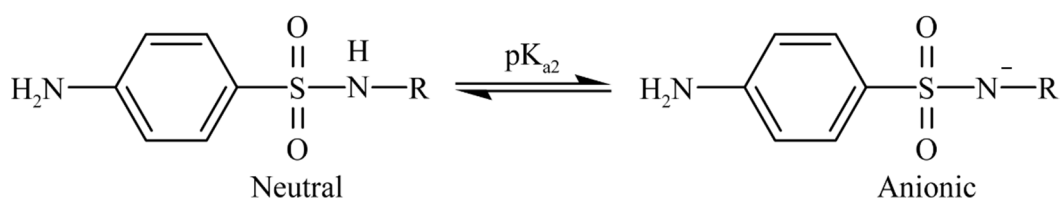
**Table 1.** Specific parameters of sulfonamide species in the UV system.

Sulfonamide	$\varepsilon \times 10^3$ (mol/cm)		$k \times 10^3$ (min <sup>-1</sup> )		Reference
	Neutral	Anionic	Neutral	Anionic	
SMZ	16.8	20.3	1.6	3.6	This study
SMM	17.9	24.2	3.1	9.0	
SMX	8.8	17.2	35.4	7.1	
SMZ	17.0	21.3	0.3	1.2	[34]
SMX	11.5	17.1	14.5	3.8	

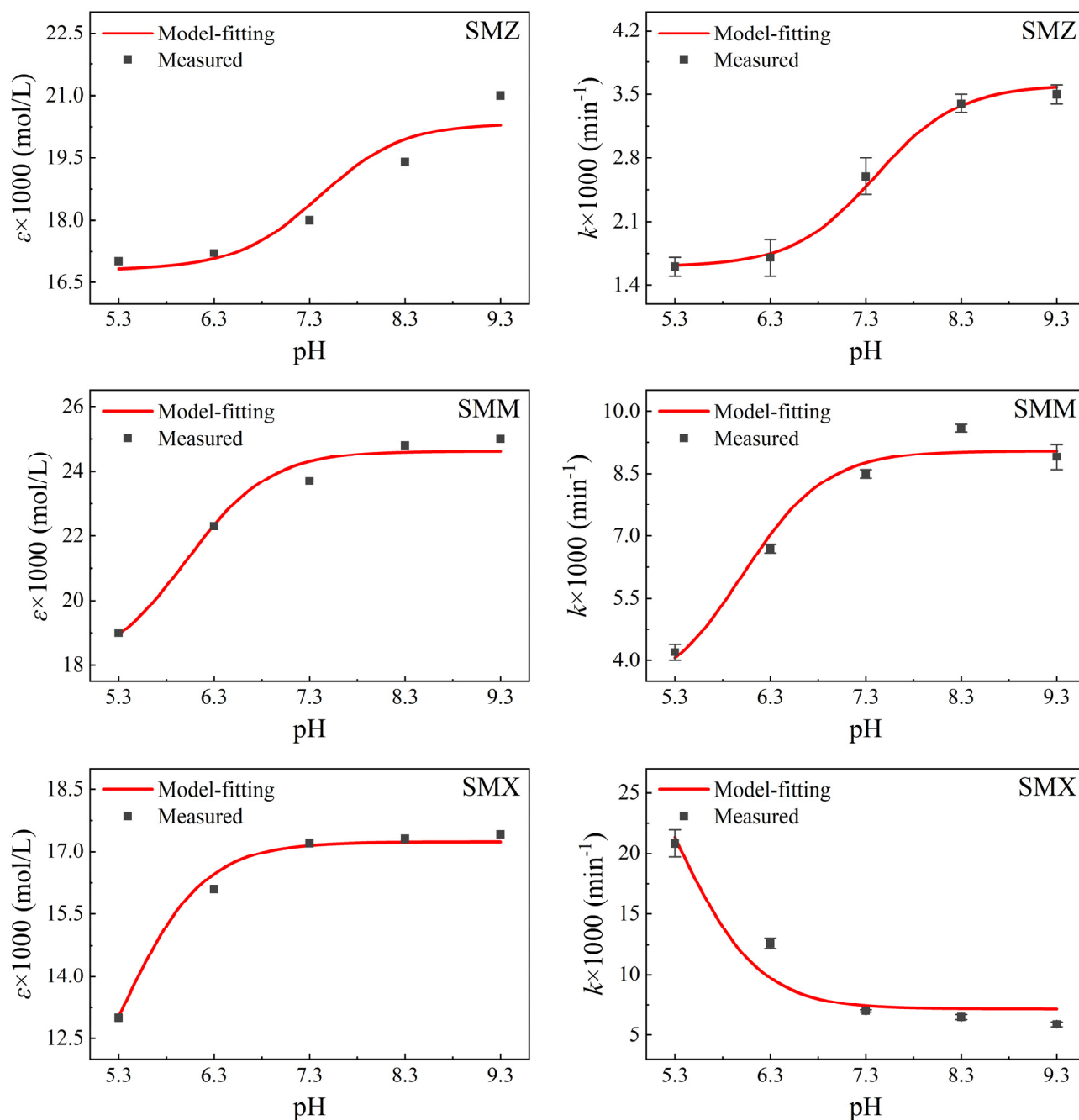
Note: The  $k$  value in reference [34] was the fluence-based photolysis rate constant (cm<sup>2</sup>/mJ).

Figure 7 shows that the overall  $\varepsilon$  and  $k$  values calculated in the experiment matched the results of model fitting well. For all three sulfonamides, higher  $\varepsilon$  values were found for anionic species compared to neutral species (Figure 5), and the overall  $\varepsilon$  values increased with increasing pH at 254 nm, as also reported by Baeza [37]. This was due to the sulfinol group ( $-\text{S}(=\text{O})_2-\text{NH}-$ ) in sulfonamides, which constantly deprotonate to liberate their lone-pair electrons in an auxochrome (N atom) when the pH increases (Scheme 1). This has a hyperchromic effect on the absorption of sulfonamides [34]. It also means that anionic species would have higher absorbance (higher  $\varepsilon$ ), with the specific  $\varepsilon$  values of sulfonamides species in Table 1 confirming this.

The specific  $k$  value of sulfonamide species (Table 1) could explain their changes during treatment in the UV system (Table 1). This could be due to sulfonamides with a five-membered heterocycle (SMX) having higher electron densities in the heterocyclic rings than those with a six-membered heterocycle (SMZ, SMM), which agrees with Lian [34]. Both SMZ and SMM were more associated with anionic species, whereas SMX was dominated by neutral species. As previously reported, for most sulfonamides, the  $k$  values increased as the pH increased. A small number of sulfonamides, e.g., SMX, have been shown to exhibit more rapid degradation under acidic conditions than under alkaline conditions [34,37,38], which is consistent with our results.



**Scheme 1.** Schematic diagram of a transition from a neutral to anionic sulfonamide species.



**Figure 7.** Results of model fitting or measurement for the sulfonamides.

### 2.5.3. Electrochemical Oxidation of Sulfonamides

To determine the influence of pH on the free chlorine yield, an experiment was conducted in the E system, in which the pH was controlled within a certain range ( $\pm 0.2$ ) without sulfonamides. The free chlorine yield increased as the pH increased (Figure 8a), which could explain the changes of the free chlorine concentration in the E system. However, the free chlorine concentration in the UV-E system was higher than that in the E system, except at pH 9.3, and there was no detection of free chlorine in the UV system (Figure 8b). This meant that chlorine consumption was different in the UV-E system, which affected the UV/chlorine conversion reactions (Equations (15)–(19)). This may be due to the existence of a competitive reaction between sulfonamides (and their products) and UV irradiation or free chlorine, which decreases the consumption of free chlorine. Additionally, there was a higher

concentration of free chlorine in the E system under alkaline conditions than in the UV-E system, which was attributed to the higher molar absorption coefficient of  $\text{OCl}^-$  compared to  $\text{HOCl}$ . The proportion of  $\text{OCl}^-$  increased as the pH increased, consequently leading to a higher photodecay (UV/chlorine conversion) rate and reducing the concentration of free chlorine compared with the E system [39].

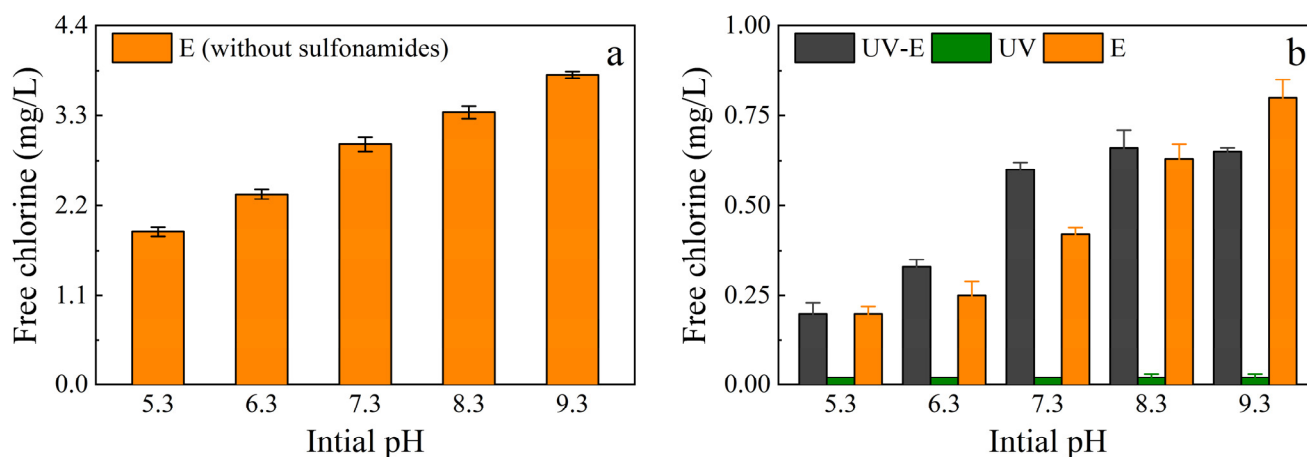


**Figure 8.** Free chlorine concentrations under different pH conditions at 120 min. (a) The free chlorine yield without sulfonamides under different pH conditions. (b) The free chlorine concentration in different treatment systems under various pH conditions.

In the E system, the  $k$  value of the three sulfonamides (Figure 5) could be further explained by considering the ratio of  $\text{HOCl}$  and  $\text{OCl}^-$  under different pH conditions (Figure 6d). Previous studies have shown that  $\text{HOCl}$  has a higher reaction rate with anionic vs. neutral sulfonamide species [28], and  $\text{HOCl}$  is more reactive than  $\text{OCl}^-$ , with the result that the effect of  $\text{OCl}^-$  could be negligible [40–42]. Therefore, the more that  $\text{HOCl}$  reacted with the anionic sulfonamide species, the better the effectiveness of the system. The anionic sulfonamide species increased with pH, whereas for  $\text{HOCl}$ , the opposite pattern was observed. Therefore, the stronger oxidizability of  $\text{HOCl}$  relative to  $\text{OCl}^-$  was not obvious in this experiment. The impact of free chlorine ( $\text{HOCl}$ ,  $\text{OCl}^-$ ) was important, as discussed in previous sections. This could be related to the disposal method because free chlorine is generated in situ by electrolysis, whereas in other systems, a reagent ( $\text{NaOCl}$ ) is typically added [28,40–42]. Because the formation of free chlorine and the reactions with sulfonamides occurred simultaneously in this experiment, the overall reaction rate was slower than direct reaction with excess free chlorine. In addition, the free chlorine yield increased as the pH increased, and anodic direct electrochemical oxidation also occurred, which further decreased the relevance of the relationship between the degradation rate constant ( $k$ ) and pH. This could explain why the optimal pH for sulfonamide degradation was 7.3 or 8.3 (neutral or alkaline conditions), and account for the lack of a clear downward trend for the decrease in the proportion of  $\text{HOCl}$  with pH under alkaline conditions.

#### 2.5.4. Sulfonamide Degradation by UV Irradiation Combined with Electrochemical Oxidation

In the UV-E system, the removal mechanism was complicated due to the existence of free chlorine conversion reactions, and the reactivity of active radicals ( $\bullet\text{OH}$ ,  $\bullet\text{Cl}$ ,  $\bullet\text{ClO}$ , and  $\bullet\text{Cl}_2^-$ ) with different organic compounds has been shown to differ substantially [43]. Additionally, the concentration of these active radicals changes as the pH changes. As previously reported, the estimated steady-state  $\bullet\text{OH}$  concentration decreased as the pH increased during the UV/chlorine treatment process, whereas the  $\bullet\text{Cl}$ ,  $\bullet\text{ClO}$ , and  $\bullet\text{Cl}_2^-$  concentrations followed the opposite pattern, with considerable reactivity with olefins and benzene derivatives [43]. Both  $\bullet\text{OH}$  and  $\bullet\text{Cl}$  are effective for the degradation of

benzoic acid, but the effect of other active radicals (e.g.,  $\bullet\text{Cl}_2^-$ ) is negligible [17]. Therefore, further investigations are required to determine whether the active species produced by UV photolysis conversion could have a promotional effect on sulfonamide degradation.

An additional control experiment was conducted, with the results shown in Figure 9. The free chlorine yield under UV irradiation decreased substantially over the duration of the experiment (over 90% at 120 min without sulfonamides), indicating the presence of UV/chlorine conversion reactions (Equations (15)–(19)). However, both the UV-E and E systems had a higher free chlorine yield than did in the UV-E system without sulfonamides. This could be attributed to the sulfonamides reacting with free chlorine and decreasing the amount of electrogeneration; hence, the conversion of free chlorine to reactive chlorine species might have been restrained due to the presence of sulfonamides.

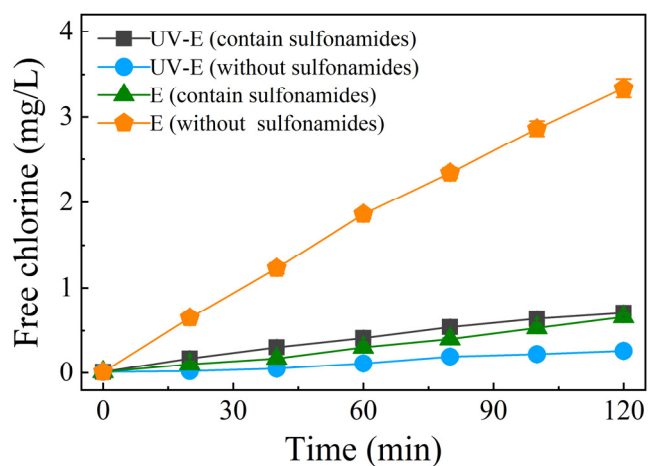


**Figure 9.** The free chlorine yield with different treatments (with or without sulfonamides). Conditions:  $\text{Cl}^-$  concentration of 50 mg/L, no aeration, UV power of 48 W, current of 1.8 A (4.8 mA/cm<sup>2</sup>), and initial pH of 8.3.

Through the comparison of  $k$  values (Table 2) for the UV-E system and UV + E, it was apparent that there was no additional promotion of SMZ degradation in the combined system (UV-E system), and the SMX degradation rate was similar under all conditions except pH 8.3. By contrast, there was a promotional effect on SMM degradation, as confirmed by the  $\Delta$  values. The results showed that the active radicals produced by the UV/chlorine process exhibited different reactivity with the sulfonamides under various pH conditions.

**Table 2.** The  $k$  values in different treatment systems (values under “UV + E” are the sums of the  $k$  values in the UV and E systems,  $\Delta$  is the difference in the  $k$  values between the UV-E system and UV + E).

Sulfonamide	$k \times 10^3 \text{ (min}^{-1}\text{)}$								
	SMZ			SMM			SMX		
	UV-E	UV + E	$\Delta$	UV-E	UV + E	$\Delta$	UV-E	UV + E	$\Delta$
pH 5.3	6.5	7.8	−1.3	9.5	10.1	−0.6	24.3	26.5	−2.2
pH 6.3	7.2	8.6	−1.4	12.3	13.4	−0.9	18.7	20.3	−1.6
pH 7.3	9.8	11.9	−2.1	16.2	15.8	0.4	16.5	18.0	−1.5
pH 8.3	12.4	13.7	−1.3	17.7	16.8	0.9	16.8	16.7	0.1
pH 9.3	10.7	13.4	−2.7	14.9	15.2	0.3	14.8	16	−2.2
Average $\Delta$	-	-	−1.76	-	-	0.02	-	-	−1.48

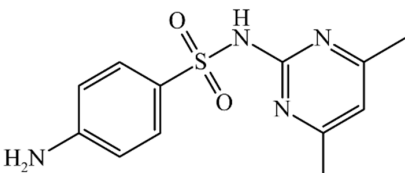
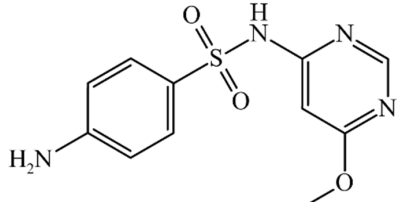
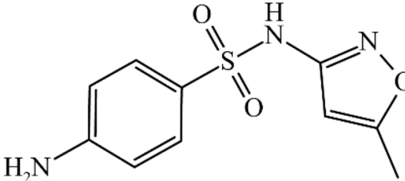
### 3. Materials and Methods

#### 3.1. Materials

##### 3.1.1. Chemicals

Veterinary sulfamethazine (SMZ) and sulfamonomethoxine (SMM) tablets were purchased from Shangdong Ease Animal Pharmaceutical Co., Ltd., Qingdao, China. Compound sulfamethoxazole (SMX) tablets (each tablet contained 25 mg of SMX and 5 mg of trimethoprim) were purchased from Shandong Zhengmu Biological Pharmaceutical Co., Ltd., Linyi, China. Standard solutions of SMZ (99%), SMM (>93.0%), and SMX (98%) were obtained from Shanghai Aladdin Biochemical Technology Co., Ltd., Shanghai, China. Detailed information on the sulfonamides is shown in Table 3. Concentrated sulfuric acid (95~98%), sodium chloride ( $\geq 99.8\%$ ), and sodium hydroxide ( $\geq 96\%$ ) were purchased from Sinopharm Chemical Reagent Co., Ltd., Shanghai, China. Titanium dioxide (TiO<sub>2</sub>) powder (Degussa P-25, 80% anatase and 20% rutile) and zinc oxide (ZnO) powder (99.7%, particle size  $50 \pm 10$  nm) were provided by Aladdin Chemistry Co., Ltd., Shanghai, China. Ultrapure/deionized water was prepared with an ultrapure water purification system (Chengdu Ultrapure Technology Co., Ltd., Chengdu, China).

**Table 3.** Structure and physicochemical parameters of the sulfonamides used.

Sulfonamides	Structure	Chemical Formula	Molecular Weight	pKa [44]
Sulfamethazine (SMZ)		C <sub>12</sub> H <sub>14</sub> N <sub>4</sub> O <sub>2</sub> S	278.33	pK <sub>a1</sub> = 2.30 pK <sub>a2</sub> = 7.40
Sulfamonomethoxine (SMM)		C <sub>11</sub> H <sub>12</sub> N <sub>4</sub> O <sub>3</sub> S	280.30	pK <sub>a1</sub> = 2.00 pK <sub>a2</sub> = 6.01
Sulfamethoxazole (SMX)		C <sub>10</sub> H <sub>11</sub> N <sub>3</sub> O <sub>3</sub> S	253.28	pK <sub>a1</sub> = 2.10 pK <sub>a2</sub> = 5.30

##### 3.1.2. Reactor Materials

A UV and electrochemical reactor incorporating flat ceramic microfiltration membranes was prepared (Figure 10). UV light was provided by six low-pressure mercury lamps (254 nm, TUV 8W/G8 T5 UVC lamp, Philips Lighting Co., Amsterdam, Poland) each equipped with a quartz glass water jacket. Mesh electrodes (thickness 2 mm, dimensions 20 × 20 cm [reticular part] and 20 × 1 cm [flat part]) were used for electrochemical oxidation. The Ti/RuO<sub>2</sub>-IrO<sub>2</sub> anode and Ti cathode (both purchased from Baoji Changli Special Metal Co. Ltd., Baoji, China) were connected to a direct current (DC) power supply (SD-500H-24, Hangzhou Kerui Electronics Co., Ltd., Hangzhou, China) for galvanostatic electrolysis. The UV lamps and electrodes were fixed using polypropylene stents. Two flat ceramic microfiltration membranes (250 × 500 × 6 mm, Shangdong Sicer Membrane Materials Co., Ltd., Zibo, China) were applied to both sides of the UV lamps and electrodes. The effluent was filtered through the flat membranes with the flow produced by a self-priming pump (JR-7442, Ningbo Jinqirui Electronic Commerce Co., Ltd., Ningbo, China).

connected to polypropylene pipes. The reactor was self-made with polypropylene and had dimensions of 62 cm (length), 42 cm (width), and 42 cm (height). An aeration device was placed in the bottom of the reactor and was connected to polypropylene aerator pipes. The reactor was also fitted with an air compressor (LJ-1530, Taizhou Bedair Electromechanical Co., Ltd., Taizhou, China).

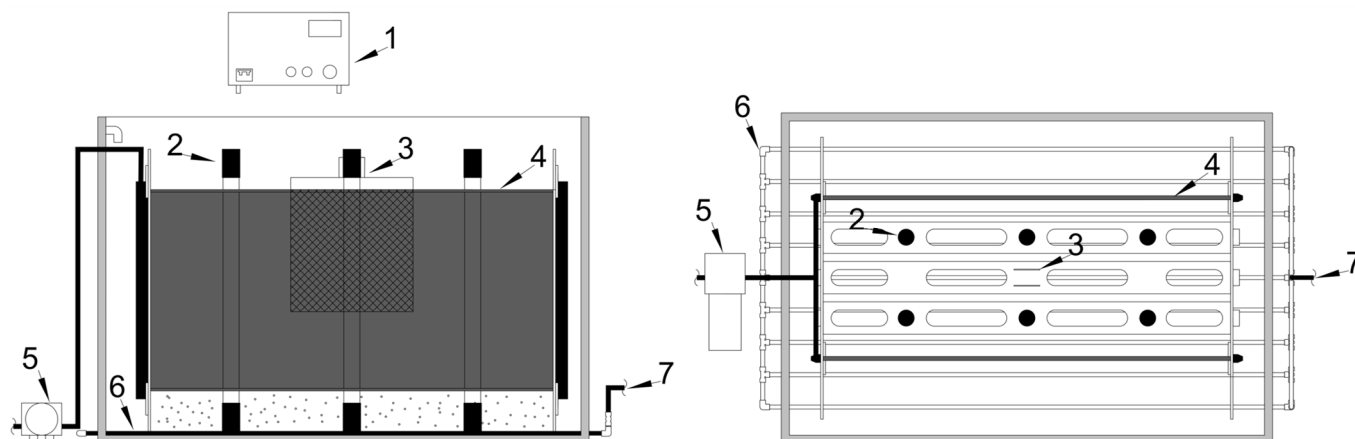


**Figure 10.** Schematic of the UV/electrochemical oxidation/flat membrane reactor (left: front view, right: top view). 1: DC power supply, 2: UV lamp (six lamps in total, each covered by a quartz glass water jacket), 3: electrode, 4: flat ceramic microfiltration membrane, 5: self-priming pump, 6: aeration device, 7: connection to an air compressor (not shown in the diagram).

### 3.2. Experimental Procedures

Using tap water, 10  $\mu\text{mol/L}$  SMZ, SMM, and SMX solutions of 70 L each were prepared in the reactor (the sulfonamide concentrations in the tablets were measured in a preliminary experiment and the available SMZ, SMM, and SMX contents were 87.7, 26.1, and 9.8 wt%, respectively). Aeration was provided with an air compressor and controlled by a gas flowmeter (DFG-6, 10~60 L/min, Darhor Technology Co., Ltd., Hangzhou, China). There were six UV lamps in total, and the UV power was controlled by the number of UV lamps in operation (each lamp was 8 W). The current was provided and controlled by a DC power supply. The effective area of each electrode plate was 376  $\text{cm}^2$ . The  $\text{Cl}^-$  concentration was controlled by adding sodium chloride, and the initial pH was controlled by adding sodium hydroxide solution or concentrated sulfuric acid. In addition, in order to evaluate the influence of suspended matter to ultraviolet light, two different concentration photocatalysts were used (0.5 g/L  $\text{TiO}_2$  and 0.1 g/L  $\text{ZnO}$ ) in the photocatalysts experiment.

The effluent was filtered through the flat membranes, with samples collected using the self-priming pump for subsequent analysis (the pump was turned on 3 mins in advance for sampling and kept off for the rest of the experiment). The experimental parameters were changed to explore the effects of different factors on antibiotic degradation. The working conditions are shown in Table 4. All experiments were conducted at room temperature ( $18.5 \pm 2$  °C). To simulate real surface water, the pH was chosen at 8.3 in first four conditions.

**Table 4.** Experimental conditions.

Condition	Aeration Rate (L/min)	Current (A)	Cl <sup>-</sup> Concentration (mg/L)	Initial pH
Aeration rate	0~55	1.0 or 1.8	20 or 50	8.3
Cl <sup>-</sup> concentration	0 or 30	1.0	20~80	8.3
		1.8		
System	0 or 30	0	50	8.3
		1.8		
Photocatalysts	30	1.8	50	8.3
		0		
		1.8		
Initial pH	0	0	50	5.3~8.3
		1.8		

### 3.3. Analytical Methods

Sulfonamides were analyzed using high-performance liquid chromatography (Essentia LC-16, Shimadzu Co., Ltd., Kyoto, Japan), with an ACE Excel 5AQ column (250 × 4.6 mm, 5 μm) used for separation. The mobile phase was an aqueous mixture of 10% acetonitrile and 0.1% formic acid with a flow rate of 1.0 mL/min. The sample injection volume was 20 μL, and the oven temperature was 30 °C. The separated components were measured using a UV-Vis spectrophotometer (UV-2550, Shimadzu Co., Ltd., Kyoto, Japan) at a detection wavelength of 258 nm. The Cl<sup>-</sup> concentration was determined using an ion meter (SevenCompact S220, Mettler Toledo Instruments Co., Ltd., Shanghai, China). The pH of the solution was determined using a portable pH meter (Smart Sensor PH828, Dongguan Wanchuang Electronic Products Co., Ltd., Dongguan, China). Free chlorine was determined using the Hach DPD method 8021 with a spectrophotometer (DR2800, Hach Co., Ltd., Shanghai, China).

Kinetics analysis of the sulfonamides was conducted as follows:

$$k = -\ln\left(\frac{c_t}{c_0}\right)/t, \quad (27)$$

where  $k$  is the pseudo-first-order kinetic rate constant of sulfonamide degradation, and  $c_0$  and  $c_t$  are the initial sulfonamide concentration and the concentration at the time of sampling, respectively.

## 4. Conclusions

The dissolved oxygen provided by aeration had only a slight effect on SMM degradation under UV irradiation. The hydraulic disturbance inhibited the electrogeneration of free chlorine and substantially decreased the degradation efficiency. A small amount of Cl<sup>-</sup> in the system produced good results, which would easily satisfy relevant wastewater discharge standards. Although photocatalysts had no promotional effect on sulfonamide degradation due to the reduction in UV penetration, because of their ability to be continuously reused and recirculated, photocatalysts still exhibit treatment potential with the application of a flat membrane. Due to their different distribution coefficients, UV irradiation had different effects on various sulfonamide species. For SMZ and SMM, anionic species were degraded at higher rates, whereas for SMX, degradation was most efficient for neutral species. The free chlorine yield increased as the pH increased, which also resulted in effective sulfonamide degradation. Free chlorine conversion reactions occurred under UV irradiation and could be restrained by sulfonamides. Reactive chlorine species promoted SMM degradation, whereas this effect was not obvious for SMZ and SMM. Compared to UV irradiation or electrochemical oxidation alone, the UV/in-situ electrochemical oxidation process was more effective for sulfonamide degradation and is suitable for the treatment of real wastewater under various environmental pH conditions.

**Author Contributions:** Conceptualization, Y.T.; methodology, G.H.; software, Z.Z.; validation, X.W.; formal analysis, Z.Z.; investigation, X.J.; resources, J.Y.; data curation, Z.Z.; writing—original draft preparation, Z.Z.; writing—review and editing, Y.T.; visualization, Y.T.; supervision, X.W.; project administration, X.W.; funding acquisition, J.Y. All authors have read and agreed to the published version of the manuscript.

**Funding:** This research was funded by the Key Laboratory of Healthy Freshwater Aquaculture (the open project Grant No. ZJK202203).

**Data Availability Statement:** The data that support the findings of this study are available from the corresponding author (X.W.), upon reasonable request.

**Acknowledgments:** Authors gratefully acknowledge the financial support from the Key Laboratory of Healthy Freshwater Aquaculture, Ministry of Agriculture and Rural Affairs, Key Laboratory of Fish Health and Nutrition of Zhejiang Province, and Zhejiang Institute of Freshwater Fisheries.

**Conflicts of Interest:** The authors declare that they have no conflict of interest.

## Appendix A

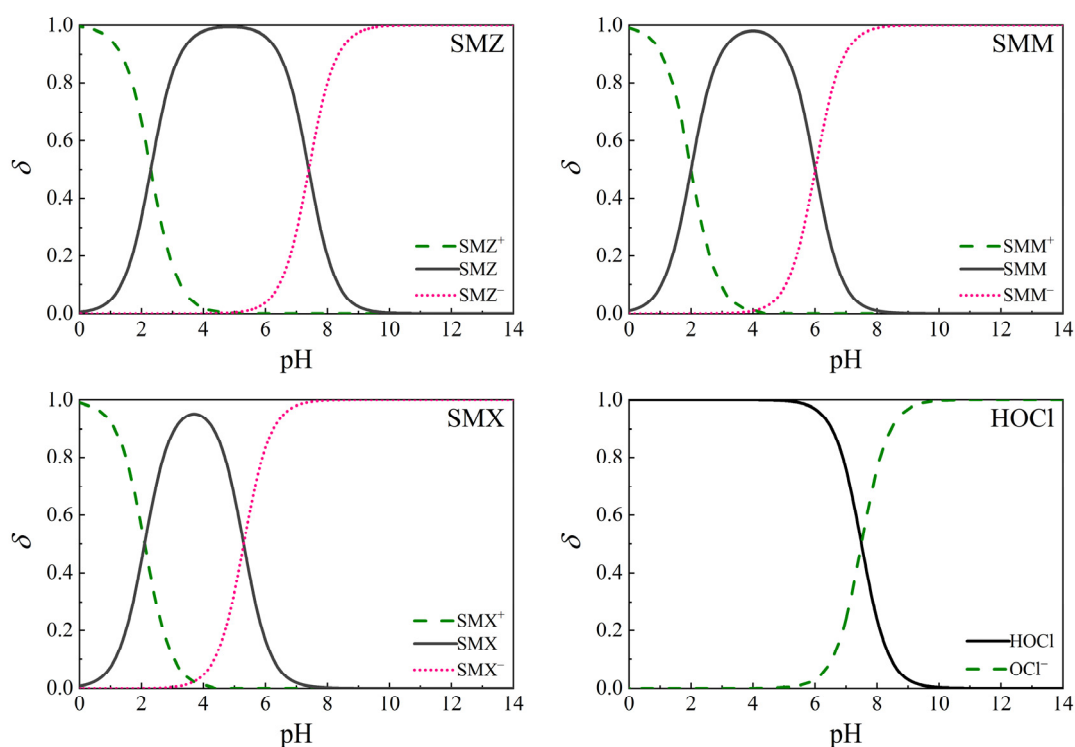


**Figure A1.** Distribution coefficients ( $\delta$ ) of sulfonamides (“+”, no mark, and “-” represent cationic, neutral, and anionic species, respectively) and HOCl at different pH. SMZ: pKa = 2.3, 7.4; SMM: pKa = 2.0, 6.0; SMX: pKa = 2.1, 5.3; and HOCl: pKa = 7.5. T = 25 °C.

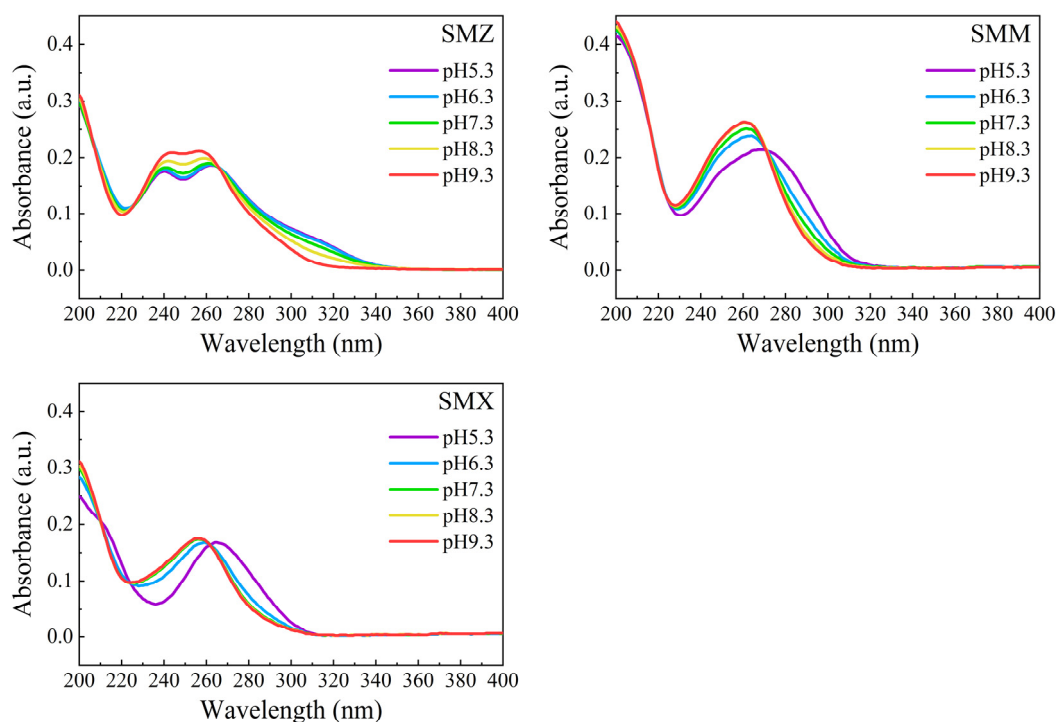


**Figure A2.** UV-vis absorption spectra of sulfonamides at various pH (the concentrations of sulfonamides were measured in 10  $\mu\text{mol/L}$ , and the measured absorbance value was deducted from the absorbance value of deionized water).

## References

- Wan, Y.; Xie, P.; Wang, Z.; Ding, J.; Wang, J.; Wang, S.; Wiesner, M.R. Comparative study on the pretreatment of algae-laden water by UV/persulfate, UV/chlorine, and UV/H<sub>2</sub>O<sub>2</sub>: Variation of characteristics and alleviation of ultrafiltration membrane fouling. *Water Res.* **2019**, *158*, 213–226. [[CrossRef](#)] [[PubMed](#)]
- Sichel, C.; Garcia, C.; Andre, K. Feasibility studies: UV/chlorine advanced oxidation treatment for the removal of emerging contaminants. *Water Res.* **2011**, *45*, 6371–6380. [[CrossRef](#)] [[PubMed](#)]
- dos Santos, A.J.; Kronka, M.S.; Fortunato, G.V.; Lanza, M.R.V. Recent advances in electrochemical water technologies for the treatment of antibiotics: A short review. *Curr. Opin. Electrochem.* **2021**, *26*, 100674. [[CrossRef](#)]
- Moreira, F.C.; Boaventura, R.A.R.; Brillas, E.; Vilar, V.J.P. Electrochemical advanced oxidation processes: A review on their application to synthetic and real wastewaters. *Appl. Catal. B Environ.* **2017**, *202*, 217–261. [[CrossRef](#)]
- Martinez-Huitle, C.A.; Brillas, E. Decontamination of wastewaters containing synthetic organic dyes by electrochemical methods: A general review. *Appl. Catal. B Environ.* **2009**, *87*, 105–145. [[CrossRef](#)]
- Ganzenko, O.; Huguenot, D.; van Hullebusch, E.D.; Esposito, G.; Oturan, M.A. Electrochemical advanced oxidation and biological processes for wastewater treatment: A review of the combined approaches. *Environ. Sci. Pollut. Res.* **2014**, *21*, 8493–8524. [[CrossRef](#)]
- Zhang, S.X.; Pang, X.F.; Yue, Z.; Zhou, Y.H.; Duan, H.T.; Shen, W.J.; Li, J.F.; Liu, Y.L.; Cheng, Q.P. Sulfonamides removed from simulated livestock and poultry breeding wastewater using an in-situ electro-Fenton process powered by photovoltaic energy. *Chem. Eng. J.* **2020**, *397*, 125466. [[CrossRef](#)]
- Martinez-Huitle, C.A.; Ferro, S. Electrochemical oxidation of organic pollutants for the wastewater treatment: Direct and indirect processes. *Chem. Soc. Rev.* **2006**, *35*, 1324–1340. [[CrossRef](#)]
- Panizza, M.; Cerisola, G. Direct and mediated anodic oxidation of organic pollutants. *Chem. Rev.* **2009**, *109*, 6541–6569. [[CrossRef](#)]
- Cominellis, C. Electrocatalysis in the electrochemical conversion/combustion of organic pollutants for waste-water treatment. *Electrochim. Acta* **1994**, *39*, 1857–1862. [[CrossRef](#)]
- Marselli, B.; Garcia-Gomez, J.; Michaud, P.A.; Rodrigo, M.A.; Cominellis, C. Electrogeneration of hydroxyl radicals on boron-doped diamond electrodes. *J. Electrochem. Soc.* **2003**, *150*, D79. [[CrossRef](#)]
- Nowell, L.H.; Hoigne, J. Photolysis of aqueous chlorine at sunlight and ultraviolet wavelengths—2. Hydroxyl radical production. *Water Res.* **1992**, *26*, 599–605. [[CrossRef](#)]
- Malpass, G.R.P.; Miwa, D.W.; Mortari, D.A.; Machado, S.A.S.; Motheo, A.J. Decolorisation of real textile waste using electrochemical techniques: Effect of the chloride concentration. *Water Res.* **2007**, *41*, 2969–2977. [[CrossRef](#)]

14. Bonfatti, F.; Ferro, S.; Lavezzo, F.; Malacarne, M.; Lodi, G.; De Battisti, A. Electrochemical incineration of glucose as a model organic substrate. II. Role of active chlorine mediation. *J. Electrochem. Soc.* **2000**, *147*, 592. [[CrossRef](#)]
15. Zhang, C.; He, D.; Ma, J.; Waite, T.D. Active chlorine mediated ammonia oxidation revisited: Reaction mechanism, kinetic modelling and implications. *Water Res.* **2018**, *145*, 220–230. [[CrossRef](#)]
16. Kishimoto, N.; Katayama, Y.; Kato, M.; Otsu, H. Technical feasibility of UV/electro-chlorine advanced oxidation process and pH response. *Chem. Eng. J.* **2018**, *334*, 2363–2372. [[CrossRef](#)]
17. Fang, J.Y.; Fu, Y.; Shang, C. The roles of reactive species in micropollutant degradation in the UV/free chlorine system. *Environ. Sci. Technol.* **2014**, *48*, 1859–1868. [[CrossRef](#)]
18. Watts, M.J.; Linden, K.G. Chlorine photolysis and subsequent OH radical production during UV treatment of chlorinated water. *Water Res.* **2007**, *41*, 2871–2878. [[CrossRef](#)]
19. Neta, P.; Huie, R.E.; Ross, A.B. Rate constants for reactions of inorganic radicals in aqueous-solution. *J. Phys. Chem. Ref. Data* **1988**, *17*, 1027–1284. [[CrossRef](#)]
20. Buxton, G.V.; Greenstock, C.L.; Helman, W.P.; Ross, A.B. Critical-review of rate constants for reactions of hydrated electrons, hydrogen-atoms and hydroxyl radicals ( $\bullet\text{OH}/\bullet\text{O}^-$ ) in aqueous-solution. *J. Phys. Chem. Ref. Data* **1988**, *17*, 513–886. [[CrossRef](#)]
21. Grebel, J.E.; Pignatello, J.J.; Mitch, W.A. Effect of halide ions and carbonates on organic contaminant degradation by hydroxyl radical-based advanced oxidation processes in saline waters. *Environ. Sci. Technol.* **2010**, *44*, 6822–6828. [[CrossRef](#)] [[PubMed](#)]
22. Shrestha, B.; Ezazi, M.; Rad, S.V.; Kwon, G. Predicting kinetics of water-rich permeate flux through photocatalytic mesh under visible light illumination. *Sci. Rep.* **2021**, *11*, 21065. [[CrossRef](#)] [[PubMed](#)]
23. Ezazi, M.; Shrestha, B.; Kim, S.I.; Jeong, B.; Gorney, J.; Hutchison, K.; Lee, D.H.; Kwon, G. Selective Wettability Membrane for Continuous Oil-Water Separation and In Situ Visible Light-Driven Photocatalytic Purification of Water. *Glob. Chall.* **2020**, *4*, 2000009. [[CrossRef](#)] [[PubMed](#)]
24. Kochkodan, V.M.; Rolya, E.A.; Goncharuk, V.V. Photocatalytic membrane reactors for water treatment from organic pollutants. *J. Water Chem. Technol.* **2009**, *31*, 227–237. [[CrossRef](#)]
25. Mozia, S. Photocatalytic membrane reactors (PMRs) in water and wastewater treatment. A review. *Sep. Purif. Technol.* **2010**, *73*, 71–91. [[CrossRef](#)]
26. Li, Y.; Yang, L.; Chen, X.; Han, Y.; Cao, G. Transformation kinetics and pathways of sulfamonomethoxine by UV/H<sub>2</sub>O<sub>2</sub> in swine wastewater. *Chemosphere* **2021**, *265*, 129125. [[CrossRef](#)]
27. Li, J.; Zhao, L.; Feng, M.; Huang, C.-H.; Sun, P. Abiotic transformation and ecotoxicity change of sulfonamide antibiotics in environmental and water treatment processes: A critical review. *Water Res.* **2021**, *202*, 117463. [[CrossRef](#)]
28. Chamberlain, E.; Adams, C. Oxidation of sulfonamides, macrolides, and carbadox with free chlorine and monochloramine. *Water Res.* **2006**, *40*, 2517–2526. [[CrossRef](#)]
29. Xin, X.; Sun, S.; Zhou, A.; Wang, M.; Song, Y.; Zhao, Q.; Jia, R. Sulfadimethoxine photodegradation in UV-C/H<sub>2</sub>O<sub>2</sub> system: Reaction kinetics, degradation pathways, and toxicity. *J. Water Process Eng.* **2020**, *36*, 101293. [[CrossRef](#)]
30. Gaya, U.I.; Abdullah, A.H.; Zainal, Z.; Hussein, M.Z. Photocatalytic treatment of 4-chlorophenol in aqueous ZnO suspensions: Intermediates, influence of dosage and inorganic anions. *J. Hazard. Mater.* **2009**, *168*, 57–63. [[CrossRef](#)]
31. Sharma, V.K.; Burnett, C.R.; Rivera, W.; Joshi, V.N. Heterogeneous photocatalytic reduction of ferrate(VI) in UV-irradiated titania suspensions. *Langmuir* **2001**, *17*, 4598–4601. [[CrossRef](#)]
32. Guo, Z.F.; Ma, R.X.; Li, G.J. Degradation of phenol by nanomaterial TiO<sub>2</sub> in wastewater. *Chem. Eng. J.* **2006**, *119*, 55–59. [[CrossRef](#)]
33. Zhang, H.-C.; Liu, Y.-L.; Wang, L.; Li, Z.-Y.; Lu, X.-H.; Yang, T.; Ma, J. Enhanced radical generation in an ultraviolet/chlorine system through the addition of TiO<sub>2</sub>. *Environ. Sci. Technol.* **2021**, *55*, 11612–11623. [[CrossRef](#)] [[PubMed](#)]
34. Lian, J.; Qiang, Z.; Li, M.; Bolton, J.R.; Qu, J. UV photolysis kinetics of sulfonamides in aqueous solution based on optimized fluence quantification. *Water Res.* **2015**, *75*, 43–50. [[CrossRef](#)] [[PubMed](#)]
35. Li, B.; Zhang, T. pH significantly affects removal of trace antibiotics in chlorination of municipal wastewater. *Water Res.* **2012**, *46*, 3703–3713. [[CrossRef](#)]
36. Zhu, G.; Sun, Q.; Wang, C.; Yang, Z.; Xue, Q. Removal of sulfamethoxazole, sulfathiazole and sulfamethazine in their mixed solution by UV/H<sub>2</sub>O<sub>2</sub> process. *Int. J. Environ. Res. Public Health* **2019**, *16*, 1797. [[CrossRef](#)]
37. Baeza, C.; Knappe, D.R.U. Transformation kinetics of biochemically active compounds in low-pressure UV photolysis and UV/H<sub>2</sub>O<sub>2</sub> advanced oxidation processes. *Water Res.* **2011**, *45*, 4531–4543. [[CrossRef](#)]
38. Boreen, A.L.; Arnold, W.A.; McNeill, K. Photochemical fate of sulfa drugs in then aquatic environment: Sulfa drugs containing five-membered heterocyclic groups. *Environ. Sci. Technol.* **2004**, *38*, 3933–3940. [[CrossRef](#)]
39. Yin, R.; Ling, L.; Shang, C. Wavelength-dependent chlorine photolysis and subsequent radical production using UV-LEDs as light sources. *Water Res.* **2018**, *142*, 452–458. [[CrossRef](#)]
40. Gonzalez, A.C.; Olson, T.M.; Rebenne, L.M. Aqueous chlorination kinetics and mechanism of substituted dihydroxybenzenes. In *Water Disinfection and Natural Organic Matter: Characterization and Control*; Minear, R.A., Amy, G.L., Eds.; ACS Symposium Series; ACS Publications: Washington, DC, USA, 1996; Volume 649, pp. 48–62. [[CrossRef](#)]
41. Gallard, H.; Von Gunten, U. Chlorination of phenols: Kinetics and formation of chloroform. *Environ. Sci. Technol.* **2002**, *36*, 884–890. [[CrossRef](#)]
42. Dodd, M.C.; Huang, C.H. Transformation of the antibacterial agent sulfamethoxazole in reactions with chlorine: Kinetics mechanisms, and pathways. *Environ. Sci. Technol.* **2004**, *38*, 5607–5615. [[CrossRef](#)] [[PubMed](#)]

43. Guo, K.; Wu, Z.; Shang, C.; Yao, B.; Hou, S.; Yang, X.; Song, W.; Fang, J. Radical chemistry and structural relationships of PPCP degradation by UV/chlorine treatment in simulated drinking water. *Environ. Sci. Technol.* **2017**, *51*, 10431–10439. [[CrossRef](#)] [[PubMed](#)]
44. Feng, M.; Baum, J.C.; Nesnas, N.; Lee, Y.; Huang, C.-H.; Sharma, V.K. Oxidation of sulfonamide antibiotics of six-membered heterocyclic moiety by ferrate(VI): Kinetics and mechanistic insight into SO<sub>2</sub> extrusion. *Environ. Sci. Technol.* **2019**, *53*, 2695–2704. [[CrossRef](#)] [[PubMed](#)]